Matthew Wall, Zhiwei Sun, and Zeyad T. Alwahabi
Quantitative detection of metallic traces in water-based liquids by microwave-assisted laser-induced breakdown spectroscopy
Optics Express, 2016; 24(2):1507-1517

Published version http://dx.doi.org/10.1364/OE.24.017384

Quantitative detection of metallic traces in water-based liquids by microwave-assisted laser-induced breakdown spectroscopy

Matthew Wall,[1] Zhiwei Sun,[2,3] and Zeyad T. Alwahabi[1,3,*]

[1]*School of Chemical Engineering, The University of Adelaide, S.A. 5005, Australia*
[2] *School of Mechanical Engineering, The University of Adelaide, S.A. 5005, Australia*
[3]*Centre for Energy Technology, The University of Adelaide, S.A. 5005, Australia*
**zeyad.alwahabi@adelaide.edu.au*

Abstract: The enhancement of laser-induced breakdown spectroscopy (LIBS) assisted with microwave radiation is demonstrated for an aqueous solution of indium using the 451.13 nm emission line. Microwave power was delivered via a near-field applicator to the LIBS measurement volume where the indium aqueous solution was presented as a liquid jet. The microwave enhancement effect was observed to decrease with increasing laser pulse fluence at 532 nm resulting in a maximum emission intensity occurring at a laser pulse fluence of 85.2 $J \cdot cm^{-2}$, independent of the microwave power used. The detection limits of indium in an aqueous solution were determined to be 10.8 ± 0.7 and 124 ± 5 ppm for the cases of microwave enhanced and standard LIBS, respectively. The 11.5-fold detection limit enhancement obtained in the liquid phase is of the same order of magnitude as that reported for other elements in solid samples, but lower than that obtained in solid phase utilizing a similar experimental setup. This establishes microwave enhancement as an effective technique for the detection of metals in aqueous solutions. In addition, the temporal evolution of plasma emission intensity was investigated and was found to be qualitatively similar to that of plasma produced from solid phase samples, which reveals the same coupling mechanism between laser generated plasma and microwave radiation.

OCIS codes: (300.6365) Spectroscopy, laser induced breakdown; (350.4010) Microwaves; (280.1545) Chemical analysis.

References and links

1. J. E. Lee, H. W. Shim, O. S. Kwon, Y.-I. Huh, and H. Yoon, "Real-time detection of metal ions using conjugated polymer composite papers," Analyst (Lond.) **139**(18), 4466–4475 (2014).
2. L. Sartore, M. Barbaglio, L. Borgese, and E. Bontempi, "Polymer-grafted QCM chemical sensor and application to heavy metalions real time detection," Sens. Actuators B Chem. **155**(2), 538–544 (2011).
3. K. Rifai, S. Laville, F. Vidal, M. Sabsabi, and M. Chaker, "Quantitative analysis of metallic traces in water-based liquids by UV-IR double-pulse laser-induced breakdown spectroscopy," J. Anal. At. Spectrom. **27**(2), 276–283 (2012).
4. S. Musazzi and U. Perini, *Laser-Induced Breakdown Spectroscopy: Theory and Applications* (Springer, 2014).
5. O. Samek, D. C. S. Beddows, J. Kaiser, S. V. Kukhlevsky, M. Liska, H. H. Telle, and J. Young, "Application of laser-induced breakdown spectroscopy to in situ analysis of liquid samples," Opt. Eng. **39**(8), 2248–2262 (2000).
6. D. W. Hahn and N. Omenetto, "Laser-induced breakdown spectroscopy (LIBS), part I: review of basic diagnostics and plasma-particle interactions: Still-challenging issues within the analytical plasma community," Appl. Spectrosc. **64**(12), 335–366 (2010).
7. Y. Feng, J. J. Yang, J. M. Fan, G. X. Yao, X. H. Ji, X. Y. Zhang, X. F. Zheng, and Z. F. Cui, "Investigation of laser-induced breakdown spectroscopy of a liquid jet," Appl. Opt. **49**(13), C70–C74 (2010).
8. M. A. Aguirre, S. Legnaioli, F. Almodovar, M. Hidalgo, V. Palleschi, and A. Canals, "Elemental analysis by surface-enhanced laser-induced breakdown spectroscopy combined with liquid-liquid microextraction," Spectrochim. Acta B At. Spectrosc. **79–80**, 88–93 (2013).

#252956 Received 1 Nov 2015; revised 10 Jan 2016; accepted 11 Jan 2016; published 19 Jan 2016

9. M. Adamson, A. Padmanabhan, G. J. Godfrey, and S. J. Rehse, "Laser-induced breakdown spectroscopy at a water/gas interface: a study of bath gas-dependent molecular species," Spectrochim. Acta B At. Spectrosc. **62**(12), 1348–1360 (2007).
10. F. A. Barreda, F. Trichard, S. Barbier, N. Gilon, and L. Saint-Jalmes, "Fast quantitative determination of platinum in liquid samples by laser-induced breakdown spectroscopy," Anal. Bioanal. Chem. **403**(9), 2601–2610 (2012).
11. P. Yaroshchyk, R. J. S. Morrison, D. Body, and B. L. Chadwick, "Quantitative determination of wear metals in engine oils using laser-induced breakdown spectroscopy: a comparison between liquid jets and static liquids," Spectrochim. Acta B At. Spectrosc. **60**(7-8), 986–992 (2005).
12. H. Ohba, M. Saeki, I. Wakaida, R. Tanabe, and Y. Ito, "Effect of liquid-sheet thickness on detection sensitivity for laser-induced breakdown spectroscopy of aqueous solution," Opt. Express **22**(20), 24478–24490 (2014).
13. S. Groh, P. K. Diwakar, C. C. Garcia, A. Murtazin, D. W. Hahn, and K. Niemax, "100% efficient sub-nanoliter sample introduction in laser-induced breakdown spectroscopy and inductively coupled plasma spectrometry: implications for ultralow sample volumes," Anal. Chem. **82**(6), 2568–2573 (2010).
14. H. Sobral, R. Sangines, and A. Trujillo-Vazquez, "Detection of trace elements in ice and water by laser-induced breakdown spectroscopy," Spectrochim. Acta B At. Spectrosc. **78**, 62–66 (2012).
15. D. H. Lee, S. C. Han, T. H. Kim, and J. I. Yun, "Highly sensitive analysis of boron and lithium in aqueous solution using dual-pulse laser-induced breakdown spectroscopy," Anal. Chem. **83**(24), 9456–9461 (2011).
16. H. Loudyi, K. Rifai, S. Laville, F. Vidal, M. Chaker, and M. Sabsabi, "Improving laser-induced breakdown spectroscopy (LIBS) performance for iron and lead determination in aqueous solutions with laser-induced fluorescence (LIF)," J. Anal. At. Spectrom. **24**(10), 1421–1428 (2009).
17. S. Koch, W. Garen, W. Neu, and R. Reuter, "Resonance fluorescence spectroscopy in laser-induced cavitation bubbles," Anal. Bioanal. Chem. **385**(2), 312–315 (2006).
18. D. W. Hahn and N. Omenetto, "Laser-induced breakdown spectroscopy (LIBS), part II: review of instrumental and methodological approaches to material analysis and applications to different fields," Appl. Spectrosc. **66**(4), 347–419 (2012).
19. B. Kearton and Y. Mattley, "Laser-induced breakdown spectroscopy: sparking new applications," Nat. Photonics **2**(9), 537–540 (2008).
20. Y. Liu, M. Baudelet, and M. Richardson, "Elemental analysis by microwave-assisted laser-induced breakdown spectroscopy: Evaluation on ceramics," J. Anal. At. Spectrom. **25**(8), 1316–1323 (2010).
21. M. Tampo, M. Miyabe, K. Akaoka, M. Oba, H. Ohba, Y. Maruyama, and I. Wakaida, "Enhancement of intensity in microwave-assisted laser-induced breakdown spectroscopy for remote analysis of nuclear fuel recycling," J. Anal. At. Spectrom. **29**(5), 886–892 (2014).
22. A. Khumaeni, T. Motonobu, A. Katsuaki, M. Masabumi, and W. Ikuo, "Enhancement of LIBS emission using antenna-coupled microwave," Opt. Express **21**(24), 29755–29768 (2013).
23. Y. Ikeda and R. Tsuruoka, "Characteristics of microwave plasma induced by lasers and sparks," Appl. Opt. **51**(7), B183–B191 (2012).
24. Y. Liu, B. Bousquet, M. Baudelet, and M. Richardson, "Improvement of the sensitivity for the measurement of copper concentrations in soil by microwave-assisted laser-induced breakdown spectroscopy," Spectrochim. Acta B At. Spectrosc. **73**, 89–92 (2012).
25. J. Viljanen, Optics Laboratory, Tampere University of Technology, FIN-33101, Tampere, Finland, Z. Sun, and Z. Alwahabi are preparing a manuscript to be called "Microwave assisted laser-induced breakdown spectroscopy at ambient conditions."
26. U. Schwarz-Schampera, "Indium," in *Critical Metals Handbook*, G. Gunn, ed. (John Wiley and Sons, 2014), pp. 204–229.
27. M. Tsujiguchi, "Indium Recovery and Recycling from an LCD Panel," in *Design for Innovative Value Towards a Sustainable Society*, M. Matsumoto, Y. Umeda, K. Masui, and S. Fukushige, eds. (Springer, 2012), pp. 743–746.
28. X. Zeng, F. Wang, X. Sun, and J. Li, "Recycling indium from scraped glass of liquid crystal display: process optimizing and mechanism exploring," ACS Sustain. Chem.& Eng. **3**(7), 1306–1312 (2015).
29. C. Maury, J. B. Sirven, M. Tabarant, D. L'Hermite, J. L. Courouau, C. Gallou, N. Caron, G. Moutiers, and V. Cabuil, "Analysis of liquid sodium purity by laser-induced breakdown spectroscopy. Modeling and correction of signal fluctuation prior to quantitation of trace elements," Spectrochim. Acta B At. Spectrosc. **82**, 28–35 (2013).
30. A. Nishiyama, A. Moon, Y. Ikeda, J. Hayashi, and F. Akamatsu, "Ignition characteristics of methane/air premixed mixture by microwave-enhanced laser-induced breakdown plasma," Opt. Express **21**(S6 Suppl 6), A1094–A1101 (2013).

1. Introduction

Metal detection in the aqueous phase in real time and *in situ* has many potential applications. Typical processes for the analysis of metal content in liquid involve sample pre-treatment and expensive equipment [1]; the ability to perform real time analysis at moderate cost through laser-induced breakdown spectroscopy (LIBS) could be of great benefit to public health through the monitoring of toxic metal concentrations in waste or drinking water [1, 2]. Applications also exist for the detection and recovery of precious metals from aqueous solutions, particularly when metals are extracted from ore by leaching [3]. This detection

#252956 Received 1 Nov 2015; revised 10 Jan 2016; accepted 11 Jan 2016; published 19 Jan 2016

could also be applied to the rapid analysis of pharmaceutical formulations and medical or forensic analyses where sample volumes are very limited [4]. The ability to perform the analysis in real time and remotely would be of significant value to the nuclear fuels industry for the analysis of nuclear wastes [5] or any industry where toxic substances must be monitored without endangering operators.

LIBS has achieved enormous popularity and has established itself as an analytical spectroscopic tool in several applications in the last decade. The popularity of this method is due to the fact that almost no sample preparation is needed along with the ability to perform *in situ* analysis in real time [5, 6], making it an ideal candidate for the previously mentioned applications. In spite of its potential benefits, liquid analysis using LIBS can result in significant problems such as poor repeatability, low sensitivity, extinction of emission, surface movements, splashing and a shorter plasma lifetime due to rapid cooling [4, 7]. Typically, the lifetimes of plasma generated in bulk liquid and plasma generated on a solid surface in gas are on the order of 1 μs and 10 ms, respectively [8], with liquid surface plasma in gas having an intermediate lifetime of around 10 μs [3, 9]. These difficulties have been partially overcome through performing LIBS on a flowing liquid sample [3, 10], a liquid jet [7, 11], a flat liquid sheet [12], a microdroplet [13] or a frozen sample [14]. All of these methods improve shot repeatability and reduce the impact of splashing by ensuring that a stable surface is presented for each laser pulse [10, 11]. Meanwhile, it is also desirable to improve limits of detection (LoDs) of LIBS in liquids for trace elements analysis.

Several methods have been recommended to improve LIBS in liquids, for example double-pulse LIBS (DP-LIBS) [3, 15], LIBS laser-induced fluorescence (LIBS-LIF) [16] and resonance-enhanced LIBS (RE-LIBS) [17]. DP-LIBS has been extensively studied in literature by Hahn and Omenetto [6, 18]. Although these methods are capable of improving the LoDs, they may require the use of a more complicated laser system. In the case of LIBS-LIF and RE-LIBS a tunable laser may be required to excite a specific atomic transition while in DP-LIBS the additional laser pulse may be generated by an additional laser or a dual-pulse laser system among other methods. These techniques are all conceptually similar as they make use of an external energy source to sustain the plasma and emission intensity. This additional energy can take the form of an additional laser pulse, but can also be supplied by microwave (MW) radiation [19].

Microwave-assisted LIBS (MW-LIBS) is a technique that has been successfully demonstrated to enhance the emission intensity of plasma by increasing the lifetime of the plasma to a few hundred μs [19–21]. The injection of microwave radiation has been accomplished by the use of an antenna [21–23] and through an enclosed microwave cavity [20, 24]. A loop-shaped antenna has been demonstrated to enhance the detection limits in gadolinium oxide of calcium by 24 times [22] and europium by 12.5 times [21]. A microwave cavity has been shown to enhance the detection limit of copper in soil by a factor of 20 [24]. Signal enhancements have also been recently demonstrated in LIBS using external microwave power at ambient condition using a near-field applicator (NFA) [25]; a 93-fold improvement in the copper limit of detection (LoD) was achieved without the need for an enclosed cavity. However, to our best knowledge, MW-LIBS has not been demonstrated on liquid phase samples. The ability to use the NFA in ambient conditions without the requirement of an enclosed cavity suggests the potential for applications in liquid phase detection.

Therefore, in the present work, MW-LIBS in liquid phase is demonstrated for the detection of aqueous indium using a near-field applicator to couple the external microwave radiation. The simplicity of the detection enhancement approach described may form the basis of a turn-key detection device in the future. Indium is a rare metal used in transparent electrodes, displays and low temperature solders [26]. Due to its rarity the recovery of indium is an important procedure, which is usually performed by leaching the indium from LCD displays into acid solutions [27, 28]. The detection of indium by LIBS has not been thoroughly investigated in literature [17, 29], possibly due to its rarity. The structure of the paper is as follows, firstly the signal enhancement effect and the plasma temporal evolution characteristics are investigated. Then the effect of laser pulse fluence and MW power on the

#252956 Received 1 Nov 2015; revised 10 Jan 2016; accepted 11 Jan 2016; published 19 Jan 2016

plasma emission intensity is investigated. Finally, quantitative detection of indium is achieved using both LIBS and MW-LIBS.

2. Materials and methods

2.1 LIBS setup

The schematic diagram of the experimental setup of MW-LIBS used in this work is presented in Fig. 1. A Q-switched Nd:YAG laser (Quantel, Brilliant B) operated at its second-order harmonic was used as the laser source (532 nm in wavelength, 10 Hz in repetition, 6 ns in duration with an initial beam width of ~3 mm). A half-wave plate coupled with a Glan-laser polarizer was used to adjust the laser pulse energy which was measured with a power meter (ES220C Pyroelectric Sensor). The laser was delivered to the measurement volume through a perforated parabolic mirror (f = 152 mm, D = 50.8 mm) and focused using a bi-convex UV fused silica lens (f = 100 mm, D = 50.8 mm). The laser was incident on the liquid jet at an angle of 15° to the vertical to reduce the impact of splashing on optical equipment [4]. The beam diameter at the focal point was estimated to be 100 μm with the focal point just below the jet surface as in previous studies [11], laser fluence calculations have been based on the estimated diameter at the focal point. The plasma emission was collected by the focusing lens, focused by the perforated parabolic mirror and directed by another lens (f = 20 mm, D = 12.54 mm) into a parabolic mirror and finally a round-to-linear 7 fiber bundle (Thorlabs, BFL200HS02). The light was then channeled into a spectrometer (Andor, Shamrock 500i, 2,400 lines/mm diffraction grating) equipped with an ICCD camera (Andor, iStar).

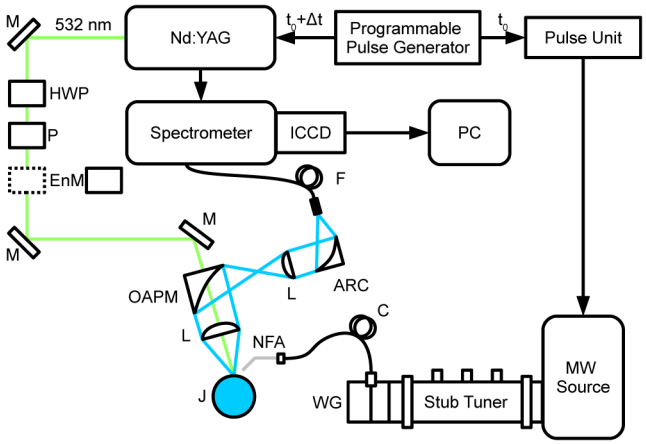

Fig. 1. Schematic of the experimental setup. M, mirror; ARC, achromatic reflective coupler; OAPM, off-axis parabolic mirror; HWP, half-wave plate; P, polarizer; EnM, energy meter; L, lens; F, fiber; C, coaxial cable; WG, waveguide-to-coaxial adapter; J, liquid jet.

2.2 Microwave setup

Pulsed MW radiation (2.45 GHz) was generated through the use of a water-cooled 3 kW Sairem MW system. The system consists of a generator coupled to an isolator equipped with a crystal detector to monitor the microwave reflected power. A WR340 waveguide was used to guide the microwave radiation to a 3-stub impedance tuner. The tuner was connected to a waveguide-to-coaxial adaptor (WR340RN), after having passed a quartz window. The waveguide-to-coaxial adaptor was attached to a 1 m flexible coaxial cable (50 ohms NN cable) with 0.14 dB @ 2.45 GHz. The end of the coaxial cable was then connected to a semi rigid cable (RG402/U). One end of the semi rigid cable was stripped off to expose ~25 mm of the inner silver plated copper steel core to form a near-field applicator (NFA). The MW radiation was coupled to the NFA which had a pointed tip with a double included angle of ~45° and was located ~0.5 mm horizontally and vertically away from the liquid jet.

#252956 Received 1 Nov 2015; revised 10 Jan 2016; accepted 11 Jan 2016; published 19 Jan 2016

The strength of microwave radiation near the tip of the NFA, was measured by a microwave survey meter (Sairem IFP 05 C). The reading at 30 mm away from the tip was 2.4 mW/cm^2, when the microwave was operating at 1.2 kW. To estimate the MW to plasma coupling efficiency, the reflected MW power was recorded. Based on the reflected MW power, it was estimated that the coupling efficiency was ~70%. It is worth noting that the microwave power reported through the paper is the direct reading of the MW power at the source. The MW duration and power were controlled using a pulse generator (Aim-TTi). The MW pulse duration was set to 1 ms and was triggered prior to the laser pulse such that the MW reached full power before the laser pulse occurred and lasted for ~700 μs afterwards before decaying.

2.3 Flow circulation system

The system used to circulate the liquid sample consisted of a peristaltic pump (Ismatec, MW-MSC 1), a pulse dampener, a circular nozzle (D = 1 mm) and a collection vessel joined by plastic tubing (Masterflex, 6485-16) as shown in Figs. 2(a) and 2(b). The operating flow rate was chosen to create a stable horizontal liquid jet (70 mL/min). It is worth noting that to date no known studies have performed LIBS on a horizontal liquid jet.

2.4 Liquid sample

A solid sample of indium trichloride ($InCl_3$) (American Elements, 99.99% purity) was used to prepare a stock solution of 1,005 ± 1 ppm indium by mass in distilled water using standard volumetric techniques. The stock solution was diluted to produce solutions with indium concentrations of 100 ± 1, 302 ± 2, 503 ± 4 and 704 ± 5 ppm. Uncertainties were taken from the equipment used and assumed to propagate such that the absolute error from the addition of two terms was the sum of the absolute errors of the terms and the relative error from the multiplication of two terms was the sum of the relative errors of the terms.

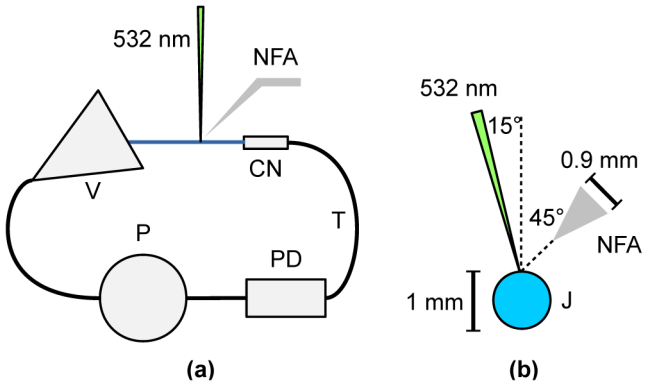

Fig. 2. Schematics showing (a) the flow circulation system and (b) the arrangement of equipment around the liquid jet. V, collection vessel; CN, circular nozzle; P, peristaltic pump; PD, pulse dampener; T, plastic tubing; J, liquid jet viewed horizontally along its propagation.

3. Results and discussion

3.1 Spectrum enhancement

Typical spectra recorded with and without microwave radiation are presented in Figs. 3 and 4. The utilized emission line of indium at 451.13 nm is from the transition of $5\ ^2P_{2/3} \leftarrow 6\ ^2S_{1/2}$, which is between the first (2,212.599 cm^{-1}) and second (24,372.957 cm^{-1}) excited states of atomic indium. The intensity of the emission line has been significantly enhanced by the external microwave, around 10 times, while the background emission remains unchanged. Figure 5 displays the normalized spectra present in Fig. 3 in order to qualitatively compare the emission line profiles. The MW-LIBS line profile does not appear to show any significant

#252956 Received 1 Nov 2015; revised 10 Jan 2016; accepted 11 Jan 2016; published 19 Jan 2016

deviation from the standard LIBS profile. This result is consistent to that achieved in a solid copper containing sample, where an enhancement of 93-fold has been demonstrated [25].

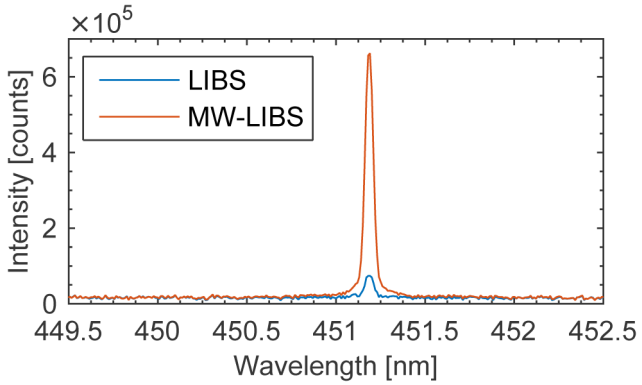

Fig. 3. Representative LIBS spectra of 1,005 ppm indium for MW-LIBS with a MW power of 1.2 kW and LIBS using a laser pulse fluence of 85.2 J·cm^{-2}, gate delay of 250 ns, gate width of 700 μs and an accumulation of 500 shots.

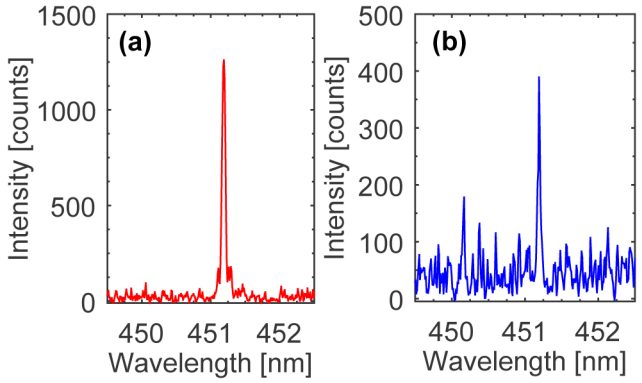

Fig. 4. Representative single shot spectra of 1,005 ppm indium for (a) MW-LIBS with a MW power of 1.2 kW and (b) LIBS with experimental parameters as in Fig. 3.

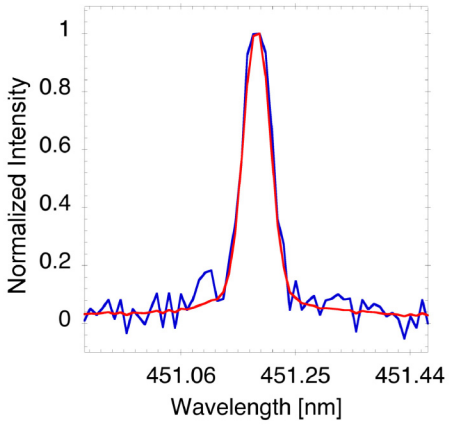

Fig. 5. Normalized spectra of 1,005 ppm indium for MW-LIBS (red) with a MW power of 1.2 kW and LIBS (blue) with experimental parameters as in Fig. 3.

#252956 Received 1 Nov 2015; revised 10 Jan 2016; accepted 11 Jan 2016; published 19 Jan 2016

3.2 Temporal evolution of MW-LIBS signal

The temporal evolution of emission intensity was investigated for both LIBS and MW-LIBS by maintaining a constant gate width and varying the gate delay for a sample of 1,005 ppm indium. The temporal evolution of MW-LIBS within 1.2 µs and 1000 µs is shown in Figs. 6(a) and 6(b), respectively. While the conventional LIBS signal decays quickly (not shown), that in MW-LIBS can be 're-ignited' by the external microwave energy at around 0.5 µs and sustained to 600 µs. For convenient interpretation of the results, the emission intensities and background intensities at each time step were extracted and are presented in Figs. 7(a)-7(d).

A strong continuum emission was present before 250 ns as can be seen in Figs. 7(a) and 7(c). The intensity of this continuum emission was not significantly increased by using MW-LIBS. Therefore, to avoid the continuum emission the gate delay was set to 250 ns for subsequent experiments (subsections 3.3 and 3.4). Figures 7(a) and 7(c) show that over a short time (0 - 600 ns) the temporal evolutions of LIBS and MW-LIBS are very similar and both quickly decay. After a delay of ~600 ns the emission signal from MW-LIBS begins to increase due to the application of MW. A possible cause of this delay is the generation of plasma with an initial electron density above the cut-off density of around 7×10^{10} cm^{-3} for microwave coupling [21, 23]. This result has been reported previously wherein delays of 10-20 µs were observed [23, 30]. As the plasma expands MW coupling with the low electron density areas of the plasma, particularly the edges of the plasma plume which have a lower electron density than the core, will become effective, reheating the plasma and increasing the emission intensity. However, there may be some delay before the plasma electron density is low enough to allow coupling with the plasma core leading to the observed delay in signal enhancement. The decrease in delay time with respect to previous studies may be due to the use of a liquid sample where the lifetime of LIBS plasma can be low due to rapid cooling. The exact mechanism of this coupling is unknown and may require further investigation. The emission signal in MW-LIBS can be seen to be sustained for the duration of the MW pulse, which is ~700 µs from the laser pulse, in Figs. 7(c) and 7(d). Previous studies have shown that microwave durations above 3 ms do not yield any significant improvement in emission intensity when applied to LIBS calcium detection in ceramics [20]. The temporal emission of MW-LIBS in liquid is qualitatively similar to that of solid phase which implies that similar interactions are present between the plasma and MW radiation in both cases.

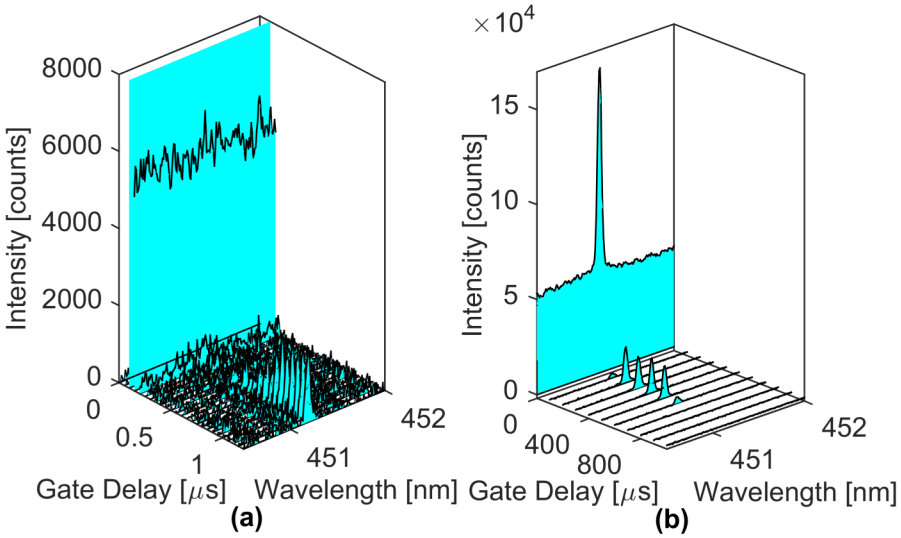

Fig. 6. MW-LIBS signal temporal evolution of 1,005 ppm indium solution at 1.2 kW MW power and 44.6 J·cm^{-2} laser pulse fluence obtained from the accumulation of 300 shots using a gate width and delay step of (a) 50 ns and (b) 100 µs.

#252956 Received 1 Nov 2015; revised 10 Jan 2016; accepted 11 Jan 2016; published 19 Jan 2016

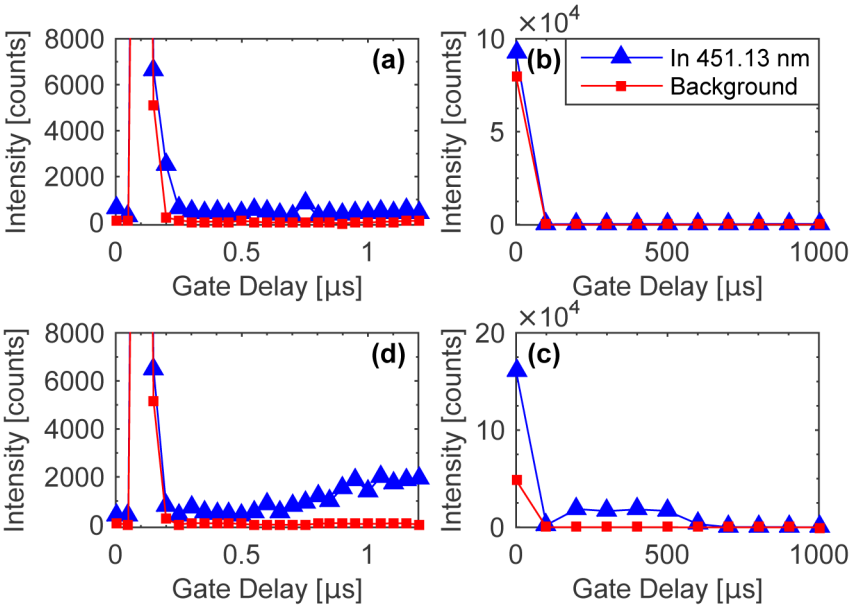

Fig. 7. (a, b) LIBS and (c, d) MW-LIBS emission intensity temporal evolution of 1,005 ppm indium solution at 1.2 kW MW power and 44.6 J·cm^{-2} laser pulse fluence obtained from the accumulation of 300 shots using a gate width and delay step of (a, c) 50 ns and (b, d) 100 μs.

3.3 Laser pulse fluence and microwave power dependence

Using a gate delay of 250 ns and a gate width of 700 μs the signal-to-noise ratio (SNR) of 1,005 ppm indium was measured at various increasing laser pulse fluence and MW power settings. The SNR was calculated as the ratio of the area integrated, background subtracted emission intensity at 451.13 nm to the standard deviation of a portion of spectrum which does not correspond to any significant emission lines (452.5 - 453.5 nm). The SNR as a function of laser fluence at different microwave powers is presented in Fig. 8.

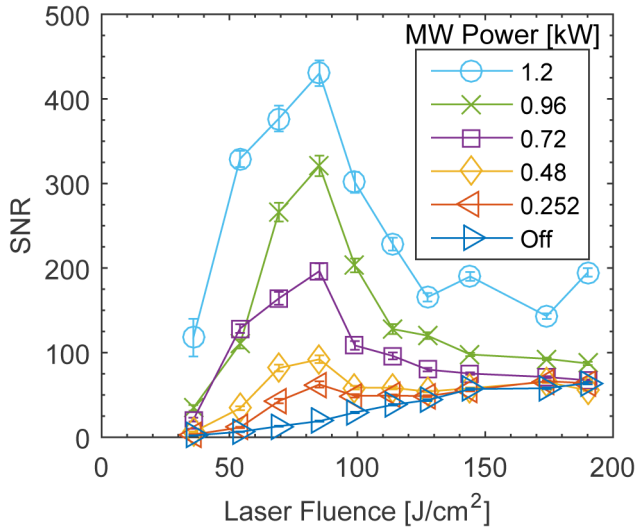

Fig. 8. MW-LIBS emission intensity for 1,005 ppm indium (451.13 nm) as indicated by SNR as a function of laser pulse fluence at various MW powers with a gate delay of 250 ns and gate width of 700 μs. Error bars are standard deviations from 500 shots.

#252956 Received 1 Nov 2015; revised 10 Jan 2016; accepted 11 Jan 2016; published 19 Jan 2016

With the MW off the SNR increased almost linearly with increasing laser power. With the presence of MW, maxima of SNR were found at the same laser fluence, ~85.2 J·cm^{-2} independent of the microwave power tested. When MW power is lower than 0.48 kW, the SNR approaches that of LIBS without MW after the maxima at 85.2 J·cm^{-2}. At higher MW powers SNR increased with increasing laser fluence until around 85.2 J·cm^{-2} where the SNR began to decrease, but was still improved over the LIBS SNR. This behavior is believed to be the result of two competing effects. In the absence of MW radiation the monotonic increase in emission intensity with laser fluence was due to the higher electron temperature of the plasma [4]. This effect is also apparent when MW radiation is applied.

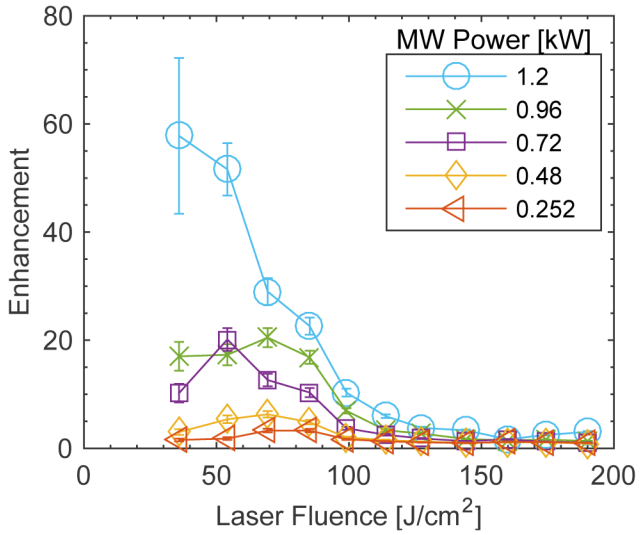

Fig. 9. MW-LIBS enhancement factors for 1,005 ppm indium (451.13 nm) as indicated by SNR ratios as a function of laser pulse fluence at various MW powers with a gate delay of 250 ns and gate width of 700 μs. Error bars are standard deviations from 500 shots.

The enhancement factors for the SNR data in Fig. 8 are presented in Fig. 9 for greater clarity, where the enhancement factor is defined as the ratio of the SNR obtained from MW-LIBS to that from LIBS. The highest enhancement factor, around 60, was obtained at the lowest laser pulse fluence of 35.7 J·cm^{-2} and quickly decreased as the laser pulse fluence was increased as seen in Fig. 9. The ability to use low fluence laser pulses also has the potential to reduce the splashing and surface motion issues associated with liquid LIBS. The enhancement was relatively low at the highest laser pulse fluence tested, only around 3 times. This is coincident with previous studies that have reported diminishing MW enhancement at higher laser fluences [20]. This may be in part due to the increase in initial plasma electron density at higher laser fluences which means that the plasma will take longer to reach the critical density for microwave coupling. The longer delay before microwave reheating of the plasma could reduce the overall emission intensity. Another potential explanation is due to the increasing volume of plasma at higher laser fluences. As the plasma becomes larger it becomes more likely that the MW radiation will not penetrate to the high electron density core of the plasma, instead re-exciting the lower electron density fringes of the plasma. As the detection elements are positioned to collect emissions from the plasma core, the lower re-excitation of the plasma core may result in an emission intensity closer to that of standard LIBS. This effect may require further investigation through imaging of the plasma and modeling of the field produced by the NFA and its interaction with the plasma. The combination of increasing emission intensity with increasing laser fluence and decreasing MW enhancement with increasing laser fluence results in a maximum SNR at ~85.2 J·cm^{-2} laser pulse fluence

#252956 Received 1 Nov 2015; revised 10 Jan 2016; accepted 11 Jan 2016; published 19 Jan 2016

(corresponding to a laser pulse energy of 6.69 mJ) that does not appear to change with MW power.

Increasing MW power appears to increase the SNR linearly in the case where the laser pulse fluence was set to 85.2 J·cm^{-2} as shown in Fig. 10. No SNR plateau is reached as the MW power is increased, implying that further enhancement may be possible with higher MW power. This result is corroborated by studies which have examined the enhancement with MW powers up to 2 kW which continue to show a near linear trend [23]. Unfortunately, the MW source utilized in this study was limited to an output of 1.2 kW precluding the investigation of higher MW powers. For subsequent experiments (subsection 3.4) a laser pulse fluence of 85.2 J·cm^{-2} and MW power of 1.2 kW were selected as these settings yielded the highest overall SNR.

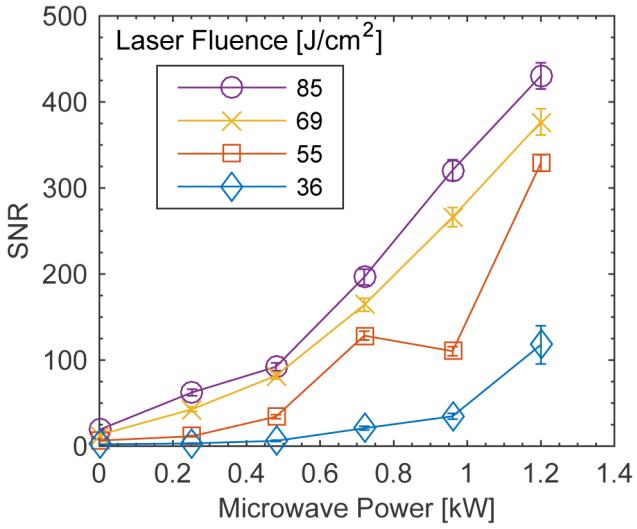

Fig. 10. MW-LIBS emission intensity for 1,005 ppm indium (451.13 nm) as indicated by SNR as a function of MW power at various laser pulse fluences with a gate delay of 250 ns and gate width of 700 µs. Error bars are standard deviations from 500 shots.

3.4 Quantitative detection of indium

Calibration curves for LIBS and MW-LIBS were generated using the prepared indium samples and optimal experimental parameters (MW power: 1.2 kW, laser pulse fluence: 85.2 J·cm^{-2}, gate delay: 250 ns, gate width: 700 us, spectral accumulation: 500 shots). The results are shown in Fig. 11, which indicates that MW-LIBS yields a higher calibration slope than LIBS. This allows for more accurate determination of sample compositions and results in a lower limit of detection. A linear function was fitted to both calibration curves using an intercept of zero, which can be seen to hold well for both MW-LIBS and LIBS at the low concentration samples. For the high concentration samples the deviation from linearity may be due to self-absorption of the indium signal. The LoD was determined by extrapolation of the calibration curves to the concentration at which the SNR was equal to 3. For MW-LIBS and LIBS the LoDs were determined to be 10.8 ± 0.7 and 124 ± 5 ppm, respectively, indicating an 11.5-fold improvement in detection limit. This liquid phase detection limit enhancement is of the same order of magnitude as that from other quantitative MW-LIBS studies for solid phase [21, 22, 24], but is lower than that from the most recent study using an NFA, where a 93-fold enhancement was reported for copper [25].

The LoD of indium is also comparable to previously reported detection limits for indium using RE-LIBS on an aluminum target in indium solution (LoD 10 ppm) [17] and LIBS on indium dissolved in liquid sodium (LoD 5 ppm) [29]. The similar LoDs are encouraging for the adoption of MW-LIBS as a liquid phase analysis technique. MW-LIBS has similar

#252956 Received 1 Nov 2015; revised 10 Jan 2016; accepted 11 Jan 2016; published 19 Jan 2016

performance to DP-LIBS, which has provided a detection limit enhancement of around 10 times for the detection of iron, lead and gold in aqueous solutions [3]. The performance of MW-LIBS lags behind LIBS-LIF which has exhibited an enhancement of two orders of magnitude for iron and lead in aqueous solutions [16]. However, it is worth noting that the use of a different LIBS setup and experimental settings makes it difficult to draw a significant conclusion from these comparisons.

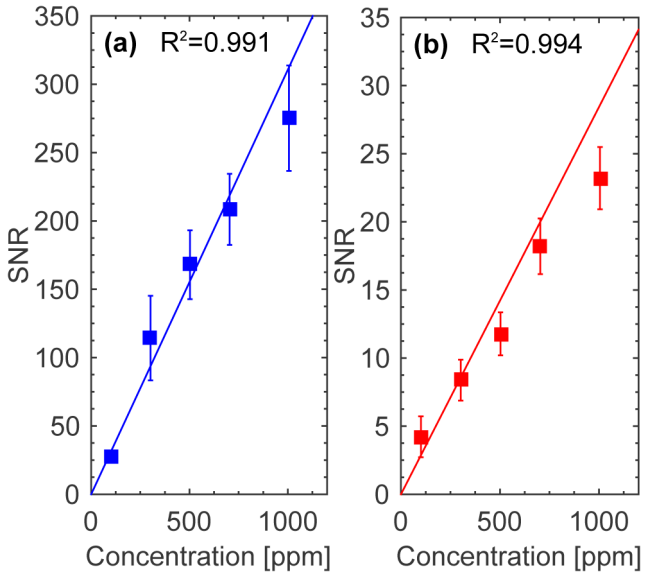

Fig. 11. Calibration curves for indium (451.13 nm) generated using (a) MW-LIBS with a MW power of 1.2 kW and (b) LIBS using a laser pulse fluence of 85.2 J·cm^{-2}, a gate delay of 250 ns and gate width of 700 μs. Error bars are standard deviations from 500 shots.

4. Conclusion

MW-LIBS has been demonstrated for the first time to be an effective technique for the detection of indium in an aqueous solution, increasing the signal emission intensity by up to 60 times and improving the LoD by 11.5 times by extending the plasma lifetime from several microseconds to several hundred microseconds. The MW enhancement was observed to be significantly influenced by the laser pulse fluence used, with decreasing enhancement being obtained as laser fluence is increased, possibly due to the formation of a higher density plasma. This yielded a maximum SNR at a laser fluence of around 85.2 J·cm^{-2}, independent of MW power. The use of a low laser fluence also has the potential to reduce the water splashing issue associated with liquid samples. Increasing MW power was observed to increase the SNR at each laser power with no maximum limit being reached indicating that the use of MW powers above 1.2 kW may yield further enhancement. Hence, MW-LIBS is a promising technique for the detection of aqueous metals with a performance comparable to that of DP-LIBS and potential applications in the detection and recovery of precious metals or the monitoring of toxic metal concentrations in water.

Acknowledgments

The financial support from the Institute for Mineral and Energy Resources (IMER) and the Faculty of Engineering, Computer & Mathematical Sciences (ECMS) of the University of Adelaide is gratefully acknowledged (SRI 2014 University of Adelaide Grant 13114264).

#252956 Received 1 Nov 2015; revised 10 Jan 2016; accepted 11 Jan 2016; published 19 Jan 2016